Journal of Alloys and Compounds 509 (2011) 4701–4706

Contents lists available at ScienceDirect

Journal of Alloys and Compounds

journal homepage: www.elsevier.com/locate/jallcom

Investigation of the hydrogen gas sensing properties of nanoporous Pd alloy films based on AAO templates

Nevin Taşaltın[a,b], Sadullah Öztürk[a], Necmettin Kılınç[a], Zafer Ziya Öztürk[a,*]

[a] Gebze Institute of Technology, Science Faculty, Department of Physics, P.K. 141, 41400 Gebze, Kocaeli, Turkey
[b] Koç University, Department of Physics, 34450 Istanbul, Turkey

ARTICLE INFO

Article history:
Received 16 February 2010
Received in revised form 13 January 2011
Accepted 15 January 2011
Available online 22 January 2011

Keywords:
Hydrogen sensor
Pd–Ag
Pd–Cu
AAO template
Palladium alloy
Nanoporous film

ABSTRACT

In this study, the hydrogen sensing properties of nanoporous Pd–Ag and Pd–Cu alloy films based on anodic aluminum oxide (AAO) templates were investigated at various temperatures (25–100 °C) and hydrogen with concentrations in the range between 250 and 5000 ppm in high purity nitrogen to determine the temperature–sensitivity relationship. A hexagonally shaped AAO template of approximately 50 nm in diameter and 10 μm in length was fabricated as a substrate for supporting a nanoporous Pd alloy film with an approximate thickness of 80 nm. The morphologies of the AAO template and the Pd alloy films were studied by scanning electron microscopy (SEM). The hydrogen sensing properties of the nanoporous Pd–Ag and Pd–Cu alloy films were measured using a transient resistance method. The sensor responses of the nanoporous Pd–Ag and Pd–Cu films on the AAO template were better than the traditional Pd–Ag and Pd–Cu thin film sensors; the sensitivities of the sensors were approximately 1.6% and 1.2%, respectively, for 1000 ppm H_2, and the detection limit was 250 ppm at room temperature. The highest sensitivity was measured at room temperature for all alloy nanoporous sensors, and the sensitivity of the Pd–Ag nanoporous alloy was higher than that of the Pd–Cu nanoporous alloy.

1. Introduction

In many industries, such as the chemical industries (refining crude oil, plastics, and reducing environment in float glass), food industry (hydrogenation of oils and fats), semiconductor industry (as processing gas in thin film deposition and in annealing atmosphere) and transportation (as fuel in fuel cells, rockets for space vehicles) hydrogen is one of the most useful gases. However, there are a number of problems, that arise from the increasing the usage of hydrogen. It is not easy to store due to its low mass, high diffusivity, and extremely low liquefaction point. As the hydrogen molecule is so small, it is hard to seal against leaks. Hydrogen leaks must be avoided, as the gas is highly flammable in the concentration range above 4% by volume in air [1]. To detect the hydrogen leakage gas at concentrations below the lower explosion limit in air of 4% at room temperature is extremely important for safety. The various types of hydrogen sensors that have been explored include metal oxide semiconductor, thermoelectric, Schottky diode, fiber optic, electrochemical, surface acoustic wave (SAW), nanomechanical and resistive palladium (Pd) sensors [2–23]. Among the hydrogen sensitive materials, Pd has a unique property of interaction with hydrogen gas. Partial pressure change of hydrogen gas determines Pd's physical properties like mass, volume and electrical resistance by forming Pd–H hydride. Pure Pd thin film sensor has two major problems. 'Peeling off' phenomenon limits durability of the thin film sensor. Too slow response could not allow real-time monitoring of gas. High sensing limit towards hydrogen reduces sensitivity at low partial pressure of hydrogen gas. Nanostructured Pd and its alloys are applied to hydrogen sensor to overcome these problems. Nanostructured Pd and its alloys can have the faster response and lower hydrogen detection limit, due to very high surface-to-volume ratio. Nanosized material has large surface area and advantages for improvement of sensor performance. Fabrication of nanosized sensor has been a matter of interest.

Nanostructures are expected to play a key role in sensor technologies. The occurring surface effects, small-size effects, and even quantum effects severely affect the physical and chemical properties of these nanosized materials. Nanostructures have recently attracted the attention of scientists for their potentiality to overcome the limitations of current hydrogen sensors due to their small size. Recently, a nanoscale hydrogen sensor has been proposed, and the researchers have developed nanostructured sensitive materials for hydrogen gas sensor applications [2–6,9,12,19–23] that have been used in the widest concentration detection region (0.01 ppm to 100%) and have a short response time (less than a few min). Detection of parts per million (ppm) (in units of mol fraction) at low hydrogen concentrations is necessary for hydrogen sensors, with a

* Corresponding author. Tel.: +90 262 6051306; fax: +90 262 6538490.
E-mail address: zozturk@gyte.edu.tr (Z.Z. Öztürk).

0925-8388/$ – see front matter © 2011 Elsevier B.V. All rights reserved.
doi:10.1016/j.jallcom.2011.01.081

dynamic range of the sensor range extending up to the explosion limit.

It was found that the most favorable site for the hydrogen location is the octahedral site in the Pd lattice [24]. The absorption of molecular hydrogen by palladium to form Pd–H hydride can cause physical property changes including mass, volume and electric resistance, all of which can be used to signal the H_2 partial pressure changes. However, although pure palladium-based hydrogen sensors have high sensitivity to H_2 gas, there are some drawbacks associated with the use of pure palladium metal. The phase transition from α phase of palladium to β phase hydride occurs at low H_2 concentrations at room temperature. In addition, the response time ranging from several to more than 10 min for Pd sensors is too slow. To overcome these problems, the sensing material has been modified by adding a second metal to make a Pd alloy for H_2 detection. Pd alloys are more suitable for hydrogen detection due to their good physicomechanical strength, their resistance to poisoning by other chemical species and their lower consumption of noble metal for a reduced fabrication cost. Baba et al. [25] studied the interaction of Pd and Pd alloys with hydrogen gas and found that the electrical resistance of the Pd and Pd alloys was dependent on the amount of hydrogen absorbed by the metal phase. Although Pd and Pd alloys as H_2 sensing materials were reported by many research groups [16–23,26–32], further improvement is still required with respect to selectivity, sensitivity of the sensors. Also, Barlag et al. [33] demonstrated that the integrated coordination number of hydrogen atoms absorbed into the H–Ti alloy system is close to 1. On the other hand, it was almost 5 for H–Pd. These results suggest that the majority of hydrogen atoms absorbed into the octahedral sites consist of at least one Ti atom. Moreover, the integrated coordination number in H–Cr is almost zero. They have suggested that when the alloying metals have a higher hydrogen solubility compared to Pd, they act as 'traps' for hydrogen in the Pd crystal. However, further investigations for various kinds of Pd alloys are required to more clearly understand the various complicated phenomena in the hydrogen absorption behavior in Pd alloys. In this sense, Pd–Ni is the most studied sensing material for hydrogen sensing. As was reported by Hughes and Schubert [26], a Pd–Ni based sensor detects hydrogen gas in the concentration range of 0.1–100% H_2 at room temperature. Cheng et al. [27] and Huang et al. [28] deposited a Pd–Ni thin film on Al_2O_3 substrates to detect hydrogen at room temperature. The response time of the sensor was typically several tens of seconds. The hydrogen sensitivity of the sensor decreased sharply with increasing temperature. Lee et al. studied hydrogen sensing properties of Pd–Ni alloy films with varying Ni content and discussed them in light of structural deformations [29]. Kumar and Malhotra [30] prepared a palladium-capped samarium film hydrogen sensor. It showed reasonable sensitivity to about 200 ppm H_2 with a response time varying from 6 to 30 s. Furthermore, Pd–Mg amorphous and Pd–Cu–Si thin films alloys have also been investigated for hydrogen detection [31,32]. Recently, the Pd–Ag has drawn renewed attention for hydrogen detection because of its high hydrogen selectivity and permeability [34–36]. Also, only a few reports described hydrogen sensing properties of the Pd–Cu alloy [37]. Such studies are currently in progress.

In this study, the hydrogen sensing properties of nanoporous Pd–Ag and Pd–Cu films on AAO templates are reported in details at various temperatures (25–100 °C) in a range of 250–5000 ppm hydrogen concentration. To explain the hydrogen sensing mechanism of the fabricated Pd alloy sensors, we used the results of the influence of Ag and Cu components on the diffusion behavior.

2. Experimental procedures

The AAO template was fabricated using a two-step anodization of an Al foil. The anodization was performed in a 0.3 M oxalic acid ($H_2C_2O_4$) solution by using a voltage of 40 V at the temperature of 5 °C. Then, the anodically grown aluminum oxide films were selectively removed by dipping the samples into a dilute phosphoric acid (H_3PO_4) solution. The second anodization was performed under the same conditions as the first. The details of the fabrication two-step anodization method were given in our previous articles [38,39]. Then, the nanoporous surface of the AAO template was used as a substrate for supporting the nanoporous Pd–Ag (15 wt.% Ag) or Pd–Cu (15 wt.% Cu) alloy film with an approximate thickness of 80 nm, which was deposited using a Leybold Univex 450 evaporator system.

The morphologies of the AAO template and nanoporous Pd alloy films coated on the AAO template were studied by scanning electron microscopy (SEM). SEM investigations were performed on a Jeol JSM 6335-SEM instrument operating at 20 kV.

The hydrogen detection apparatus was composed of a flow-type aluminum chamber, with a heatable sample holder, a temperature controller (Lakeshore 340), a multimeter (Fluke 8846A), a mass flow control unit (MKS) and gas cylinders. For the hydrogen detection experiment, the sensors were placed in the temperature-controlled chamber where various concentrations of H_2 in high purity nitrogen (250–5000 ppm with a total flow rate of 200 sccm) were introduced. The volume of the measurement chamber was 1 L. Two Au pad electrodes were contacted on the top of the surface of the nanoporous Pd–Ag and Pd–Cu alloy films. Prior to the measurement, we performed several cycles of evacuation and refilling high purity nitrogen for purging the measurement chamber. For adjusting the desired hydrogen concentration, 5000 ppm hydrogen gas tube that was diluted with high purity nitrogen (99.999%) was used as a hydrogen gas source. The relative humidity was measured as lower than 1% during the gas sensing measurements. Using this source and high purity nitrogen as carrier gas, the concentrations of hydrogen in this work were adjusted with mass flow controllers between 250 and 5000 ppm. So, gas sensing properties of the nanoporous Pd–Ag and Pd–Cu alloy films were measured using a resistance transient method. For determination of the hydrogen sensing properties, a desired concentration of H_2 in high purity nitrogen as carrier gas was introduced into the chamber; resistance–time (R–t) characteristics of the sensor were measured *in situ* at various temperatures (25 °C, 50 °C, 100 °C). All measurements data were recorded using an IEEE 488 data acquisition system incorporated to a personal computer.

3. Results and discussion

The fabricated AAO template [39] and the nanoporous Pd–Ag and Pd–Cu films were characterized by SEM. Fig. 1a and b shows a typical top view and cross-sectional view of the AAO template, Fig. 1c and d shows the top views of the Pd–Ag and Pd–Cu thin films coated on the AAO template, respectively.

As shown in Fig. 1, pores in the fabricated AAO template are approximately 50 nm in diameter with 80 nm interpore distances (Fig. 1a) and 10 μm lengths (Fig. 1b). Also, as shown in Fig. 1c and d, the morphology of the coated nanoporous Pd alloy films with 80 nm thickness on the AAO templates are almost the same as that of the AAO templates. We calculated the AAO nanopore density approximately 1.2×10^{10} cm^{-2} (the nanopore density ρ is given as $2/\sqrt{3}\,D_{\text{int}}^2 \times 10^{14}$ cm^{-2}, where D_{int} is the interpore distance) [40]. As the surface areas of the nanoporous Pd–Ag and Pd–Cu films coated on the AAO templates are very high, we expected that these nanoporous Pd alloy films would detect hydrogen gas very fast and with a high sensitivity to low hydrogen concentrations (as low as 250 ppm).

The hydrogen sensing mechanism of Pd and Pd alloys could be explained as follows: The first process, adsorption, is often the rate limiting step in the overall reaction. As the sensing responses of the Pd–Ag and Pd–Cu films are indeed a process of hydrogen adsorption/dissociation on the surface and then diffusion into the film, increasing the quantity of surface adsorption sites or dissociation areas of the Pd–Ag and Pd–Cu films will result in enhanced absorption of H in the Pd–Ag and Pd–Cu films. The nanoporous Pd–Ag and Pd–Cu films provide very large surface areas, which are beneficial for the rapid adsorption/desorption of hydrogen gas and its diffusion into the nanoporous Pd–Ag and Pd–Cu films. This causes a change in the electronic properties of the structure, which then causes a resistance shift in the resistance–time (R–t) transients. This shift and change can be readily measured and, with appropriate calibration, indicate the concentration of hydrogen. Barlag et al. [33] reported a simple model that was called a "*two-state model*" for describing the diffusion behavior of H_2 in Pd–Ag and Pd–Cu

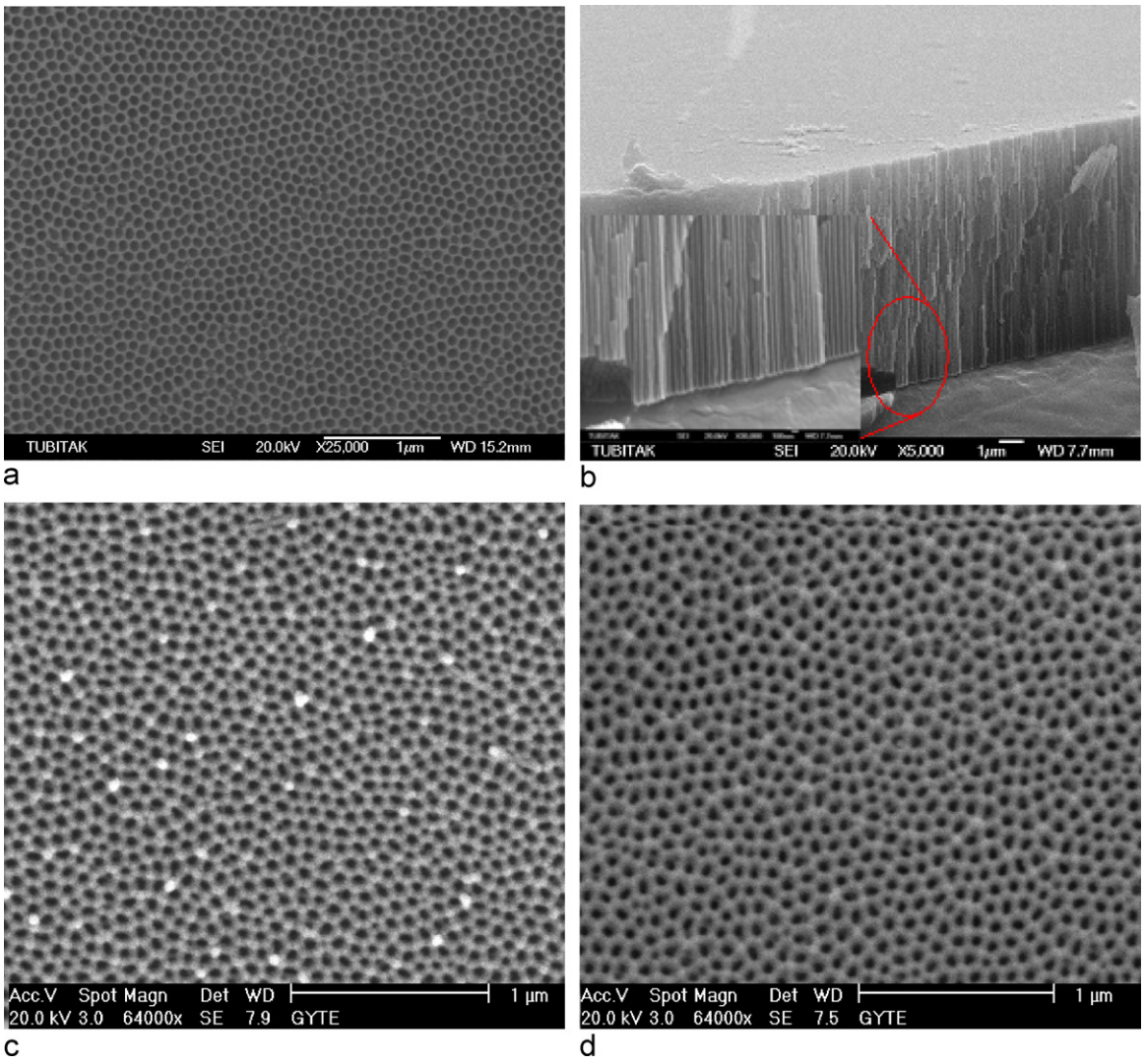

Fig. 1. SEM images of the top view of the AAO template (a), cross-sectional view of the AAO template (b), top view of the Pd–Ag thin film coated on the AAO template (c), and top view of the Pd–Cu thin film coated on the AAO template (d).

alloys, and in this paper we used this model to explain the hydrogen sensing mechanism of the fabricated Pd alloy sensors. When H_2 molecule sticks on the Pd alloy surface, physisorption occurs. The molecule is held to the surface by Van der Waals force with 10–20 kJ/mol bonding energy. Then H_2 molecule dissociates with the interaction of sp or d wavefunction of the atom of the Pd with the 1s wave function of the hydrogen atom. The energy associated with the interaction is sufficient to break H–H bond. After dissociation, the H atom diffuses into the Pd alloy and tends to occupy interstitial sites. In this study, according to the literature, above 50 K, in Pd alloys with fcc (face centered cubic) lattice, hydrogen atoms tend to occupy the octahedral interstitial sites by jumping over the potential barrier separating the interstitial sites. In Pd alloy crystal; there are two types of octahedrals, Pd octahedrals and octahedrals of the adding metal (Ag, Cu). Thus, the result of the reaction of the H and Pd alloy, the Pd–Ag–H system and Pd–Cu–H system are formed. In Pd–Ag–H and Pd–Fe–H systems, for the jumping of the H atom, as it is hydrogen diffusion coefficient is higher than adding metals', the octahedral interstitial sites of the Pd are more favorable for hydrogen occupation. Accordingly, different activation energies exist for jumps from one site into a neighboring one in the alloy. The activation energies for jumping between the octahedrals of the Ag, Cu and Pd are different. Since the hydrogen diffusion coefficient of the Pd atoms is higher than Ag or Cu atoms, in Pd–Ag–H system hydrogen atom wants to move between Pd–Pd octahedrals or Ag–Ag octahedrals, in Pd–Cu–H system hydrogen atom wants to move between Pd–Pd octahedrals or Cu–Cu octahedrals. Thus, Ag or Cu octahedrals play trap role in the Pd alloy lattice, H atoms jump over the adding metals. Also, as a result of the hydrogen gas sensing, while H atoms occupying the Pd octahedrals by jumping Ag or Cu octahedrals, the lattice constant of Pd alloy crystal is expand compare to Pd alloy that in nitrogen ambient. Also, for Pd alloys, the lattice expansion is higher than the lattice expansion of the pure Pd as the Pd alloy consists of adding metal traps. As a result of all these explanations, when hydrogen atoms diffuse in Pd–Ag and Pd–Cu alloy films, the resistance of the films much more increase than Pd films. Therefore, resistance variation of the nanoporous Pd–Ag and Pd–Cu films upon absorption of hydrogen is higher than nanoporous Pd films. The resistances of the nanoporous Pd alloy films were measured *in situ* at various temperatures with exposure to different concentrations of H_2.

Fig. 2a shows the resistances versus time for the Pd–Ag and Pd–Cu nanoporous film sensors on AAO templates during exposure to 250–5000 ppm H_2 at room temperature. After 250 ppm H_2 was exposed to the nanoporous Pd–Cu alloy sensor, the resistance of the sensor increased rapidly from 82.7 Ω to a maximum value of

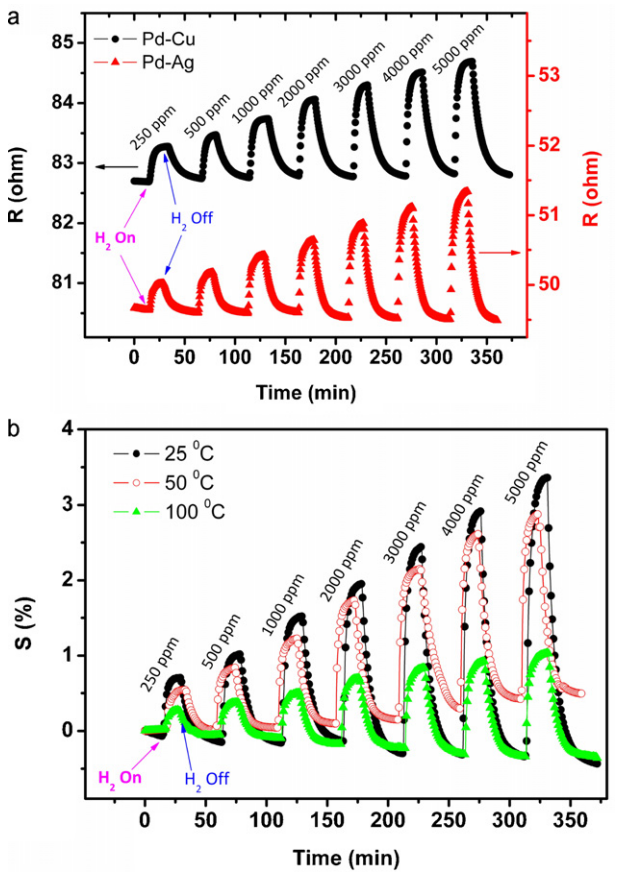

Fig. 2. Resistance versus time for nanoporous Pd–Cu and Pd–Ag alloy film sensors exposed to 250–5000 ppm H_2 in high purity N_2 at room temperature (a), and the typical behavior of the sensor response upon exposure to 250–5000 ppm H_2 in high purity N_2 as a function of time for the nanoporous Pd–Ag alloy sensor at different temperatures (b).

83.27 Ω in a few minutes, as seen in the left scale of Fig. 2a. Similarly, when 250 ppm H_2 was exposed to the nanoporous Pd–Ag alloy sensor, the resistance of the sensor increased rapidly from 49.66 Ω to a maximum value of 50.02 Ω in a few minutes, as seen in the right scale of Fig. 2a. When 250 ppm H_2 was exposed to the sensors, the resistance changes of the sensors were 0.54 Ω and 0.36 Ω for the nanoporous Pd–Cu and Pd–Ag alloy sensors, respectively. The baseline resistance and the resistance change of the nanoporous Pd–Cu alloy sensor were higher than those of the nanoporous Pd–Ag alloy sensor for the indicated H_2 concentrations. For both the nanoporous Pd–Cu and Pd–Ag alloy sensors, after reaching saturation the sensors were purged with 200 sccm high purity N_2. After purging with N_2, the resistance of both alloy sensors decreased sharply in 10 min, reaching a steady state value as seen in Fig. 2a. A similar behavior was obtained for other H_2 concentrations. The resistance changes increased with increasing concentration for both nanoporous Pd–Cu and Pd–Ag alloy sensors at room temperature, as given in Fig. 2a. The nanoporous Pd–Cu and Pd–Ag alloy sensors were totally reversible, and the limit of detection (LOD) of the sensors was 250 ppm at room temperature. The increase in the resistance of Pd alloy sensors with exposure to H_2 gas could be explained as follows: adsorption of molecular H_2 on the Pd alloy films, dissociation of the molecule leading to formation of H atoms, migration of H atoms into the Pd alloy film, and reaction between H and Pd or (Ag and Cu) atoms leading to formation of a hydride [41]. In addition, it has been known that the resistance of this hydride increases.

The sensing properties of a nanoporous alloy sensor can be assessed by determining the sensor response, which is defined as:

$$S(\%) = \frac{\Delta R}{R_0} \times 100 \quad (1)$$

where ΔR is the change in resistance and R_0 is the reference value (baseline) of the sensor. In order to obtain the temperature dependence of the sensor response, the sensing properties were measured at 25 °C, 50 °C, and 100 °C. Fig. 2b shows the sensor response versus time for the nanoporous Pd–Ag film sensor on the AAO template upon exposure to 250–5000 ppm H_2 at different temperatures. At the indicated temperatures, the response rapidly increased to a maximum after the 250 ppm H_2 exposure to the sensor. Then, after purging with 200 sccm high purity N_2, the response decreased sharply to the baseline. A similar behavior was obtained for other H_2 concentrations (500–5000 ppm). The sensor response decreased with increasing temperature for all desired H_2 concentrations, as seen in Fig. 2b. For instance, the sensor response decreased from 1.68 to 0.6 for 1000 ppm H_2 exposure to the nanoporous Pd–Ag sensor with increasing temperature from 25 °C to 100 °C, respectively. The decrease in the sensor response with increasing temperature is explained with Sieverts' law, which states that the logarithm of hydrogen solubility increases linearly with inverse temperature [26,33,34]. It is well known that the absorbtion of hydrogen on Pd follows the Sieverts' law, according to which the amount of hydrogen absorbed is a function of the hydrogen partial pressure;

$$\left(\frac{\mathrm{H}}{\mathrm{Pd}}\right)_{\mathrm{at}} = K_S \cdot \sqrt{p_{H_2}} \quad (2)$$

where $(H/Pd)_{at}$ is the atom ratio of H and Pd components, K_S the Sieverts constant, and p_{H_2} is the hydrogen partial pressure in Pa. The temperature dependence of the Sieverts constant is described by an Arrhenius-type equation:

$$\ln K_S = \frac{\Delta_S S}{R} - \frac{\Delta_S H}{RT} \quad (3)$$

where $\Delta_S S$ and $\Delta_S H$ are the entropy and the enthalpy of solution, respectively, T the temperature, and R the molar gas constant. On the other hand, sensor response increased with increasing concentration at a desired temperature, as seen in Fig. 2b. Similarly to that for the nanoporous Pd–Ag sensor, temperature-dependent sensing behavior was observed for the nanoporous Pd–Cu sensor. Sensor responses of the nanoporous Pd–Cu sensor were 1.19, 1.05 and 0.55 for 1000 ppm H_2 exposure at the temperatures of 25 °C, 50 °C, and 100 °C, respectively. It was observed that the sensor response of the nanoporous Pd–Cu sensor is lower than the response of the nanoporous Pd–Ag sensor at all indicated temperatures and for all H_2 concentrations. This result can be confirmed according to the diffusivity calculations of the previous study [33].

Fig. 3 shows the sensor responses of the nanoporous Pd–Ag and Pd–Cu film sensors as a function of concentration at various temperatures. The maximum sensor responses were obtained at room temperature for both nanoporous Pd–Ag and Pd–Cu sensors. The sensor responses increased with increasing concentration of H_2 in the range from 250 to 5000 ppm at desired temperatures for both nanoporous Pd–Ag and Pd–Cu sensors, as seen in Fig. 3. Except at room temperature for the nanoporous Pd–Ag sensor, a nonlinear relationship between the sensor response and concentration was obtained at 25 °C, 50 °C, and 100 °C for the two sensors.

Similarly, at room temperature for the nanoporous Pd–Ag sensor, the sensor response appeared to saturate for high concentrations of H_2; on the other hand, the sensor response of the nanoporous Pd–Ag sensor was higher than the sensor response of the nanoporous Pd–Cu sensor at the indicated temperatures. For instance, the sensor responses of the nanoporous Pd–Ag and Pd–Cu

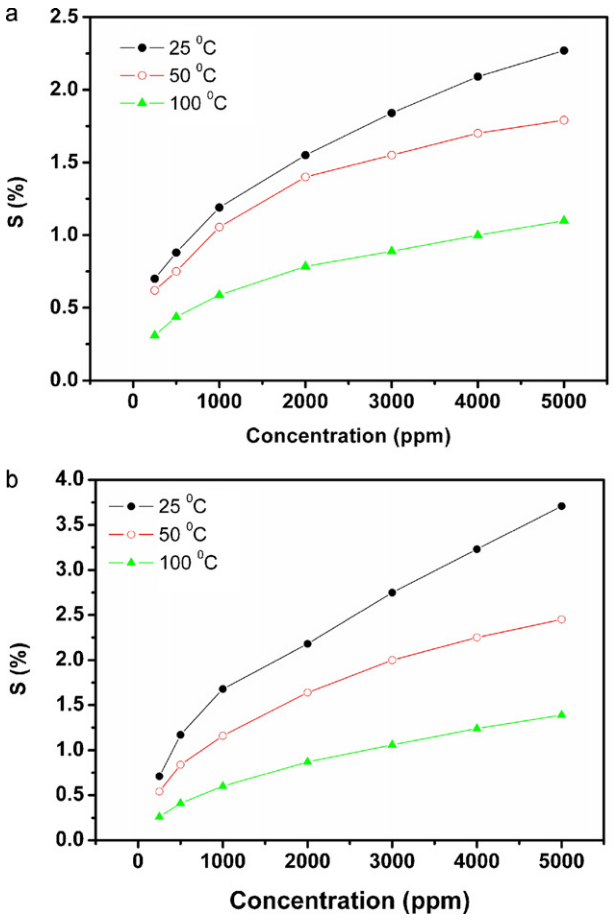

Fig. 3. The sensor responses of the nanoporous Pd–Cu alloy film sensor (a) and the nanoporous Pd–Ag alloy film sensor (b) as a function of H_2 concentration at different temperatures.

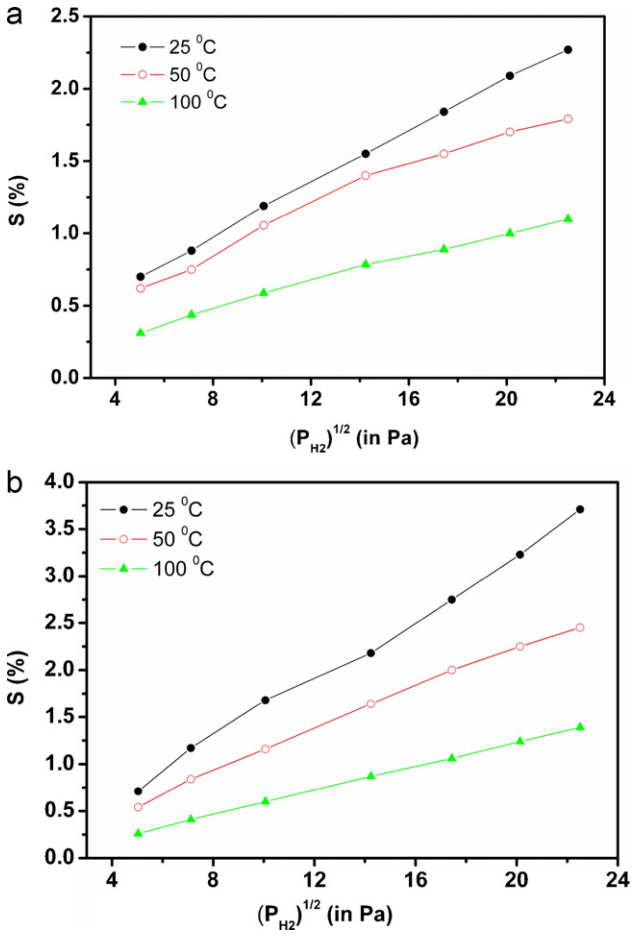

Fig. 4. The sensor response versus square root of hydrogen partial pressure at different temperatures for the nanoporous Pd–Cu (a) and Pd–Ag (b) alloy sensors.

sensors were 1.68 and 1.19, respectively, for 1000 ppm H_2 exposure at room temperature. Previously, we found that nanoporous Pd films (55 nm) based on an AAO sensor have high and reversible responses due to their enhanced absorption and desorption of hydrogen [22]. The response of the nanoporous Pd film was approximately 1.8 towards 1000 ppm H_2 at room temperature, and the response was decreased to 0.5 with an increased temperature of 100 °C. We expected to obtain a high response to H_2 for nanoporous Pd alloy films, but instead we observed lower sensor responses for nanoporous Pd–Ag and Pd–Cu sensors due to the high film thickness of the alloys.

Fig. 4 shows the sensor response versus square root of hydrogen partial pressure for the nanoporous Pd alloy sensors at different temperatures. A linear relationship between the sensor response and square root of hydrogen partial pressure was obtained at 25 °C, 50 °C, and 100 °C for the two sensors. The sensor response was decreased with increasing temperature at these partial pressure ranges for two sensors. The temperature and hydrogen partial pressure dependence of the sensor response could be explained with Sieverts' law.

4. Summary

In this study, the hydrogen sensing of nanoporous Pd–Ag and Pd–Cu films on AAO templates have been investigated at various temperatures and hydrogen gas concentrations to yield information about the temperature–sensitivity relationship. For this purpose, hexagonally ordered AAO templates were fabricated with pores of 50 nm diameters, 10 μm lengths and 80 nm interpore distances, and then a nanoporous Pd alloy films with a thickness of 80 nm was evaporated onto these templates. The temperature dependence of responses in a range of 25–100 °C was investigated for 250–5000 ppm H_2 concentrations. It was found that the sensors showed better sensitivity compared to traditional Pd alloy thin film sensors, with responses of the sensors of 1.68% and 1.19% towards 1000 ppm H_2 at room temperature for the nanoporous Pd–Ag and Pd–Cu film sensors, respectively, and the detection limit was 250 ppm for both nanoporous alloy sensors. The sensor response of the nanoporous alloy sensors decreased with increasing temperature. The advantages of the nanoporous Pd alloy sensors reported here are the fast response and small recovery time, their good mechanical strength and simple fabrication process.

Acknowledgement

This study was supported by The Scientific and Technological Research Council of Turkey. Project title: "Investigation and Development of Nanotechnologic Hydrogen Sensors" and project number "106T546."

References

[1] R.C. Weast, Handbook of Chemistry and Physics, CRC, Cleveland, 1976.
[2] O.K. Varghese, D. Gong, M. Paulose, K.G. Ong, C.A. Grimes, Sens. Actuators B: Chem. 93 (2003) 338–344.
[3] J.S. Wright, W. Lim, D.P. Norton, S.J. Pearton, F. Ren, J.L. Johnson, A. Ural, Semicond. Sci. Technol. 25 (2010) 024002.

[4] Y. Shen, T. Yamazaki, Z.F. Liu, D. Meng, T. Kikuta, J. Alloys Compd. 488 (2009) L21–L25.
[5] A. Qurashi, E.M. El-Maghraby, T. Yamazaki, Y. Shen, T. Kikuta, J. Alloys Compd. 481 (2009) L35–L39.
[6] E. Sennik, Z. Colak, N. Kilinc, Z.Z. Ozturk, Int. J. Hydrogen Energy 35 (2010) 4420–4427.
[7] G. Korotcenkov, S.D. Han, J.R. Stetter, Chem. Rev. 109 (2009) 1402–1433.
[8] N. Tasaltin, F. Dumludag, M.A. Ebeoglu, H. Yuzer, Z.Z. Ozturk, Sens. Actuators B: Chem. 130 (2008) 59–64.
[9] K. Skucha, Z.Y. Fan, K. Jeon, A. Javey, B. Boser, Sens. Actuators B: Chem. 145 (2010) 232–238.
[10] M.A. Butler, Appl. Phys. Lett. 45 (1984) 1007.
[11] T. Watanabe, S. Okazaki, H. Nakagawa, K. Murata, K. Fukuda, Sens. Actuators B: Chem. 145 (2010) 781–787.
[12] D. Monzon-Hernandez, D. Luna-Moreno, D. Martinez-Escobar, Sens. Actuators B: Chem. 136 (2009) 562–566.
[13] M. Nishibori, W. Shin, N. Izu, T. Itoh, I. Matsubara, S. Yasuda, S. Ohtani, Int. J. Hydrogen Energy 34 (2009) 2834–2841.
[14] X.M.H. Huang, M. Manolidis, C.J. Seong, J. Hone, Appl. Phys. Lett. 86 (2005) 143104.
[15] W.P. Jakubik, M.W. Urbanczyk, S. Kochowski, J. Bodzenta, Sens. Actuators B: Chem. 82 (2002) 265–271.
[16] T. Xu, M.P. Zach, Z.L. Xiao, D. Rosenmann, U. Welp, W.K. Kwok, G.W. Crabtree, Appl. Phys. Lett. 86 (2005) 203104.
[17] T. Kiefer, L.G. Villanueva, F. Fargier, F. Favier, J. Brugger, Appl. Phys. Lett. 97 (2010) 121911.
[18] M. Ramanathan, G. Skudlarek, H.H. Wang, S.B. Darling, Nanotechnology 21 (2010) 125501.
[19] F. Yang, S.C. Kung, D.K. Taggart, R.M. Penner, Sens. Lett. 8 (2010) 534–538.
[20] F. Yang, S.C. Kung, M. Cheng, J.C. Hemminger, R.M. Penner, ACS Nano 4 (2010) 5233–5244.
[21] F. Yang, D.K. Taggart, R.M. Penner, Nano Lett. 9 (2009) 2177–2182.
[22] N. Tasaltin, S. Ozturk, N. Kilinc, Z.Z. Ozturk, Appl. Phys. A: Mater. 97 (2009) 745–750.
[23] E. Sennik, N. Kilinc, Z.Z. Ozturk, J. Appl. Phys. 108 (2010) 054317.
[24] G. Alefeld, J. Völkl, Hydrogen in Metals I. Basic Properties, Springer-Verlag, Berlin, 1978.
[25] K. Baba, U. Miyagawa, K. Watanabe, Y. Sakamoto, J. Mater. Sci. 25 (1990) 3910–3916.
[26] R.C. Hughes, W.K. Schubert, J. Appl. Phys. 71 (1992) 542–548.
[27] Y.T. Cheng, Y. Li, D. Lisi, W.M. Wang, Sens. Actuators B: Chem. 30 (1996) 11–16.
[28] L. Huang, H. Gong, D.K. Peng, G.Y. Meng, Thin Solid Films 345 (1999) 217–221.
[29] E. Lee, J.M. Lee, E. Lee, J.S. Noh, J.H. Joe, B. Jung, W. Lee, Thin Solid Films 519 (2010) 880–884.
[30] P. Kumar, L.K. Malhotra, Mater. Chem. Phys. 88 (2004) 106–109.
[31] S. Nakano, S. Yamaura, S. Uchinashi, H. Kimura, A. Inoue, Sens. Actuators B: Chem. 104 (2005) 75–79.
[32] S. Kajita, S. Yamaura, H. Kimura, A. Inoue, Sens. Actuators B: Chem. 150 (2010) 279–284.
[33] H. Barlag, L. Opara, H. Züchner, J. Alloys Compd. 434 (2002) 330–332.
[34] R.R.J. Maier, B.J.S. Jones, J.S. Barton, S. McCulloch, T. Allsop, J.D.C. Jones, I. Bennion, J. Opt. A: Pure Appl. Opt. 9 (2007) 45–59.
[35] M. Wang, Y. Feng, Sens. Actuators B: Chem. 123 (2007) 101–106.
[36] R.C. Hughes, W.K. Schubert, T.E. Zipperian, J.L. Rodriguez, T.A. Plut, J. Appl. Phys. 62 (1987) 1074.
[37] R. Linke, U. Schneider, H. Busse, C. Becker, U. Schroder, G.R. Castro, K. Wandelt, Surf. Sci. (1994) 307–309.
[38] N. Tasaltin, S. Ozturk, N. Kilinc, H. Yuzer, Z.Z. Ozturk, Appl. Phys. A: Mater. 95 (2009) 781–787.
[39] N. Tasaltin, S. Ozturk, H. Yuzer, Z.Z. Ozturk, J. Optoelectron. Biomed. Mater. 1 (2009) 79–84.
[40] W. Lee, R. Li, U. Gösele, K. Nielsch, Nat. Mater. 5 (2006) 741–747.
[41] F.A. Lewis, The Palladium/Hydrogen System, Academic Press, New York, 1967.